Heliyon 10 (2024) e36145

Contents lists available at ScienceDirect

Heliyon

journal homepage: www.cell.com/heliyon

Research article

The relationship between humeral head angulation and bone void within the humeral head in proximal humerus fractures

Jiabao Ju [a,1], Yongwen Zhou [b,1], Liang Chen [c,1], Mingtai Ma [a], Yichong Zhang [a], Zhentao Ding [a], Renbin Li [d,**], Jianhai Chen [a,*]

[a] Department of Trauma & Orthopedics, Peking University People's Hospital, Beijing, China
[b] Department of Orthopedics, Affiliated Hospital of Panzhihua University, Sichuan, China
[c] Department of Orthopedics, Hospital of Traditional Chinese Medicine of Zhongshan, Guangzhou University of Chinese Medicine, Guangdong, China
[d] Department of Orthopedics, Fuzhou Second Hospital of Xiamen University, Fujian, China

ARTICLE INFO

Keywords:
Proximal humerus fractures
Three-dimensional reconstruction
Humeral head bone void
Humeral head angulation

ABSTRACT

Background: The variability of humeral head angulation in proximal humerus fractures (PHFs) is a noteworthy observation. The purpose of this study was to investigate the potential association between humeral head angulation and bone void within the humeral head in PHFs.
Methods: We used the reconstruction function in Mimics software to generate three-dimensional models of fractures. Bony landmarks were employed to accurately define the calcar and humeral head zone. Boolean subtraction was performed to calculate the volume of head bone void.
Results: The cohort consisted of 60 (74.1 %) varus, 21 (25.9 %) valgus, and 23 (22.1 %) neutral angulated PHFs. The mean percentage of humeral head bone void was 38.5 ± 17.8 in varus, 36.3 ± 15.7 in valgus, and 30.1 ± 10.6 in neutral angulated PHFs. A significant difference was observed between the varus and neutral groups (P = 0.035). In addition, an analysis of humeral head bone void was conducted among patients aged over 65 years old, revealing a mean percentage of 42.7 ± 16.4 in varus (27 cases), 34.8 ± 14.5 in valgus (13 cases), and 28.1 ± 11.8 in neutral (8 cases) angulated PHFs. The difference between the varus and neutral groups was also significant (P = 0.023).
Conclusion: All types of angulation patterns exhibited humeral head bone void to some extent, with the varus-displaced PHFs demonstrating more obvious defects in comparison to the neutral angulated type.

1. Introduction

Proximal humerus fracture (PHF) is a prevalent type of extremity fracture, representing around 5 % of all fractures and nearly 50 % of all humerus fractures [1,2]. Treatment options for PHFs include nonsurgical immobilization, internal fixation, and shoulder arthroplasty, with the choice of treatment being influenced by the type of fracture and patient health status [1,3–5]. Common complications after treatment include nonunion, displacement of greater tuberosity, humeral head necrosis, and malunion [6].

* Corresponding author.
** Corresponding author.
E-mail addresses: 892675411@qq.com (R. Li), shoudlerchen@126.com (J. Chen).
[1] These authors contributed equally.

https://doi.org/10.1016/j.heliyon.2024.e36145
Received 20 June 2023; Received in revised form 4 August 2024; Accepted 9 August 2024
Available online 10 August 2024

The injury mechanism of proximal humerus fractures is often caused by the extension of the upper limb to the ground during falls, and violence spreads along the upper limb to cause fractures. Most patients have similar mechanical mechanisms, but the direction of humeral head angulation is variable. A prior investigation found that preoperative varus deformity was linked to humeral calcar bone defect [7], and that initial varus deformity led to higher rates of complications [8]. However, fractures with preoperative varus or valgus coronal displacement were shown to have similar outcomes following endosteal fibular strut augmentation [9–11]. As a result, medial instability was identified as a strong predictor for postoperative varus malunion [12,13]. When a proximal humerus fracture occurs, the humeral head and surgical neck of the humerus divide into two parts. To maintain a good positional relationship between the two, the support of the humeral head by the calcar area of the surgical neck of the humerus is very important, and the support is mutual, and there are certain requirements for the bone mass of the humeral head. If the bone loss of the humeral head is severe and it is an empty shell, the humeral head cannot be stably supported by the humeral moment. Indeed, both medial calcar and humeral head contributed equally to maintaining medial stability, bone void within the humeral head in PHFs was not given enough consideration. Additionally, the calculation of irregular shapes made the analysis of proximal humeral bone void challenging.

Three-dimensional fracture reconstruction using Mimics software is widely used in visualizing and analyzing complex fractures in bones and other structures [14–16]. By converting medical imaging data into 3D models, it enables clinicians to better understand the geometry and biomechanics of fractures, facilitating more accurate diagnosis and treatment planning.

In our investigation, we utilized the Mimics software to conduct a detailed analysis of humeral head bone void in patients with PHFs. We employed CT-based three-dimensional reconstruction models and Boolean calculation techniques to directly visualize and quantify the extent of bone void within the humeral head and investigate their potential impact on humeral head angulation. Our findings shed light on the crucial role of humeral head bone void in providing medial stability and underscore the importance of considering bone defects in the diagnosis and treatment of PHFs. By leveraging the capabilities of the Mimics software, this study contributes to a deeper understanding of bone void within the humeral head in maintain the medial instability of PHFs and paves the way for more effective and personalized treatment strategies.

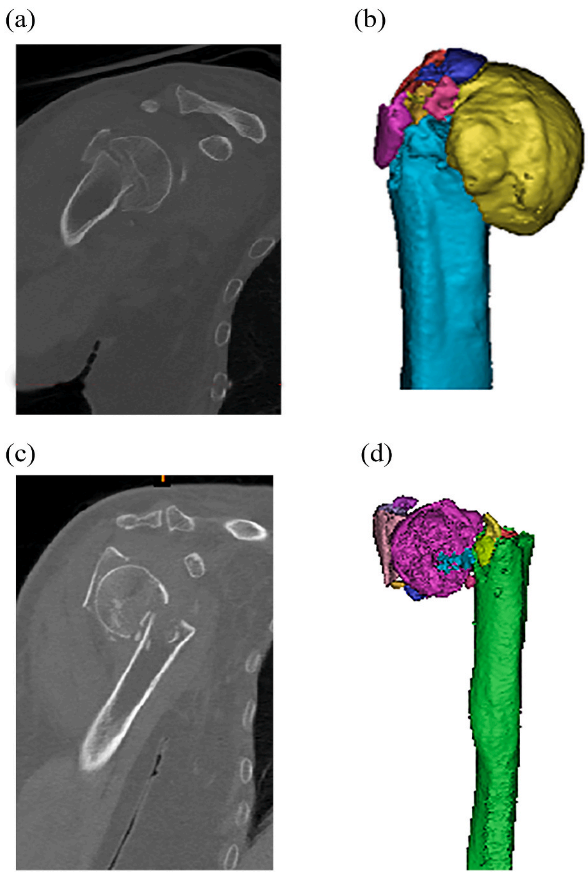

Fig. 1. CT and 3D images of a PHF with varus and valgus displaced deformity. (a)Coronal view of CT scan. (b) 3D view of reconstructed varus displaced PHF model. (c)Coronal view of CT scan. (d) 3D view of reconstructed valgus displaced PHF model.

2. Methods

Ethics approval

Our study was conducted in accordance with the ethical principles outlined in the Declaration of Helsinki. The research protocol was reviewed and approved by the Institutional Review Board of Peking University People's Hospital, Sichuan Panzhihua Hospital, and Fuzhou Hospital (2020PHB072-01). And informed consent was obtained from the patients for the publication of their CT images.

2.1. Patient characteristics

To identify all cases of PHFs for our study, we conducted a comprehensive retrospective database search across multiple medical centers, including Peking University of People's Hospital, Sichuan Panzhihua Hospital, and Fuzhou Hospital, during the period of 2019–2020. We included all patients older than 18 years old who had undergone preoperative shoulder CT scans with a slice thickness of $\leq$1 mm and excluded those with deformities or tumors to ensure the accuracy and specificity of our analysis. Our rigorous selection criteria and large-scale data collection enable us to provide a more comprehensive and representative evaluation of PHFs in the study population.

2.2. Original CT data and three-dimensional fracture models

To obtain the raw data for our study, we collaborated with the Department of Radiology at three hospitals. We then employed the Mimics software (Materialize Belgium) to import the original DICOM data to evaluate the quality of image. The CT slice width was no more than 1 mm and slice increments were within 3 mm. We analyzed CT image in three planes, and generate the three-dimensional reconstructions by using 3D reconstruction function in the Mimics software [17]. We used specific settings within the Mimics software for thresholding, including the move, zoom, mirror, translation, and rotation functions, to ensure accurate reconstruction. Each step of the manual measurement process was meticulously performed, following the standardized protocol described by Armitage and et al. [18].

2.3. Varus and valgus deformity

Due to symmetry of the left and right sides and limitation to obtain the contralateral shoulder CT scan, we used the reduced fracture model to measure the neck-shaft angle [19]. The methods described by Jeong and Pearl, which involves calculating the angle formed by the centerline of the shaft and a perpendicular line to the base of the anatomic neck, were used in our study [20,21]. We manually measured the neck shaft angle after the 3D reconstruction. Specifically, neck-shaft angles with $<130^\circ$ were classified as varus displaced (Fig. 1a and b), whereas angles $>140^\circ$ were classified as valgus angulated (Fig. 1c and d). Angles falling between 130 and 140° were classified as neutral.

2.4. Calcar and humeral head zone

To accurately define the calcar zone in our study, we utilized three distinct planes of analysis, as depicted in Fig. 2. Specifically, we identified the upper and lower boundaries of the calcar zone by locating the medial curvature below the anatomical neck and the point where the surgical neck intersects with the shaft. The posterior boundary was established as the anterior edge of the greater and lesser tuberosity [22]. To separate the humeral head from the humeral shaft for further analysis, we employed a cut function within the Mimics software, utilizing plane B as the boundary.

2.5. Calcar fracture fragments

The calcar fracture fragment was defined as an isolated fracture fragment in the calcar zone. And the volume of calcar fracture fragment was shown in the information of the fracture model in the software.

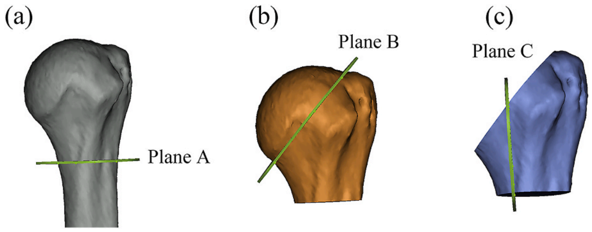

Fig. 2. Three planes to define the calcar zone. (a) Plane A corresponds to where the surgical neck intersects with the shaft. (b) Plane B corresponds to the anatomical neck. (c)Plane C corresponds to the anterior edge of greater and lesser tuberosity.

2.6. Calculation of humeral head bone void

Initially, we performed CT thresholding of the spongy bone (148–661 HU) to create a mask and reconstruct the initial 3D model. Subsequently, we used the fill cavity function of the Mimics software to fill the empty parts of the humerus, resulting in a filled 3D model. We then applied cutting plane B to obtain the original humeral head (Fig. 3 model A) and filled it to obtain a complete humeral head (Fig. 4 model B). The volume of humeral head bone void was estimated by conducting Boolean subtraction of the volume of model A from model B. The proportion of humeral head bone void was determined by dividing the volume of humeral head bone void by the volume of model B.

2.7. Statistical analysis

The study participants' demographic data and fracture characteristics were presented as means and standard deviations or proportions, and medians and quartiles or proportions, respectively. The differences of incidences of calcar fracture fragments between groups were tested using Fisher's exact test. The percentage of bone void between groups was analyzed using ANOVA to determine if the differences were significant. A p-value of less than 0.05 was considered statistically significant.

3. Results

The study cohort consisted of a total of 104 patients with PHFs, of which four were classified as Neer two-part, 57 as Neer three-part, and 43 as Neer four-part fractures. The majority of the cohort was comprised of females (n = 69, 66.3 %) with a mean age of 64.7 ± 14.1 years. Out of all PHFs, 60 (74.1 %) were classified as varus, 21 (25.9 %) as valgus, and 23 (22.1 %) as neutral angulated fractures. Further details regarding the demographic characteristics of the study population across the three groups can be found in Table 1.

Calcar fracture fragments were observed in most patients, with a higher incidence in varus angulated fractures (90.0 %) than valgus displaced fractures (52.4 %) or neutral type (73.9 %). This difference was statistically significant ($P < 0.001$) and was more pronounced between valgus and varus PHFs, as evidenced by the Bonferroni method. To determine the potential influencing factors of angulation patterns, we performed multiple logistic regression analysis, including gender, age, Neer classification, and percentage of humeral head bone void. Our analysis revealed that the percentage of humeral head bone void was significantly associated with varus deformity (odds ratio (OR) 27.38; 95 % confidence interval (CI) [1.209, 620.425]; $P = 0.038$).

The results showed that the mean percentage of humeral head bone void was 38.5 ± 17.8 in varus, 36.3 ± 15.7 in valgus, and 30.1 ± 10.6 in neutral angulated PHFs. Furthermore, we found that the difference between the varus and neutral groups was statistically significant ($P = 0.035$), as depicted in Fig. 5a. In addition, we investigated the percentage of humeral head bone void in patients aged over 65 years. The mean percentage of humeral head bone void was 42.7 ± 16.4 in varus (27 cases), 34.8 ± 14.5 in valgus (13 cases), and 28.1 ± 11.8 in neutral (8 cases) PHFs. Again, the difference between the varus and neutral groups was found to be statistically significant ($P = 0.023$), as presented in Fig. 5b. However, in patients under 65 years of age, the differences in the percentage of humeral head bone void between the three groups were not statistically significant. Table 2 displays the associations between humeral head bone void and angulation patterns. Intriguingly, six (10.0 %) varus displaced PHFs did not exhibit any calcar fracture fragments, and the mean percentage of humeral head bone void was 29.3 % in the group without calcar fracture fragment and 39.6 % in the fracrure group. Nevertheless, no statistically significant difference was observed between the two groups ($P = 0.18$).

4. Discussion

Factors influencing humeral head angulation in PHFs were still complicated. We used CT-based three-dimensional reconstruction models to analyze humeral head bone void in PHFs in our study. And we found that humeral head angulation was not only associated with calcar fractures, but also with humeral head bone void. All kinds of angulation patterns had humeral head bone void to some degree, and the defects were more obvious in the varus displaced PHFs compared to the neutral angulated. The mutual support relationship between the humeral head and the surgical neck is essential for proper fracture healing and functional recovery. Cancellous bone voids and demineralization in the humerus head area significantly affect the structural integrity of the bone, leading to instability and increased difficulty in fracture healing.

Previous studies believed that the medial calcar played an important role in fracture stability and union, and medial disruption and inappropriate neck shaft angle were associated with varus deformity and postoperative complications [23–25]. Consistent with

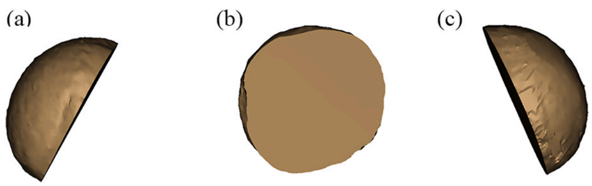

Fig. 3. 3D reconstruction and separated humeral head from the original fracture model. (a), anterior view; (b), lateral view; (c), posterior view.

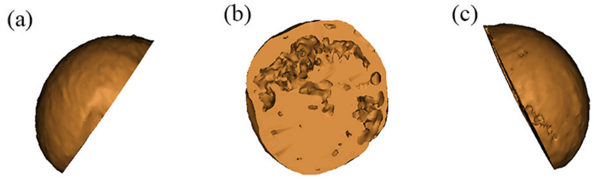

Fig. 4. 3D reconstruction and separated humeral head from the filled fracture model. (a), anterior view; (b), lateral view; (c), posterior view.

Table 1
Demographics of patients in three groups.

	Varus(n = 60)	Valgus(n = 21)	Neutral(n = 23)	*P*
Age,(mean ± sd)	65.1 ± 15.6	70.8 ± 12.3	60.1 ± 15.3	0.08
Female(n, %)	34 (56.7 %)	14 (66.7 %)	13(56.5)	0.39
Dislocation(n, %)	8(13.3 %)	3(14.3 %)	2(8.7 %)	0.82
Neer classification				**0.02**
2(n, %)	0 (0.0 %)	2 (9.5 %)	2 (8.7 %)	
3(n, %)	31 (51.7 %)	9 (42.9 %)	17 (73.9 %)	
4(n, %)	29 (48.3 %)	10 (47.6 %)	4 (17.4 %)	

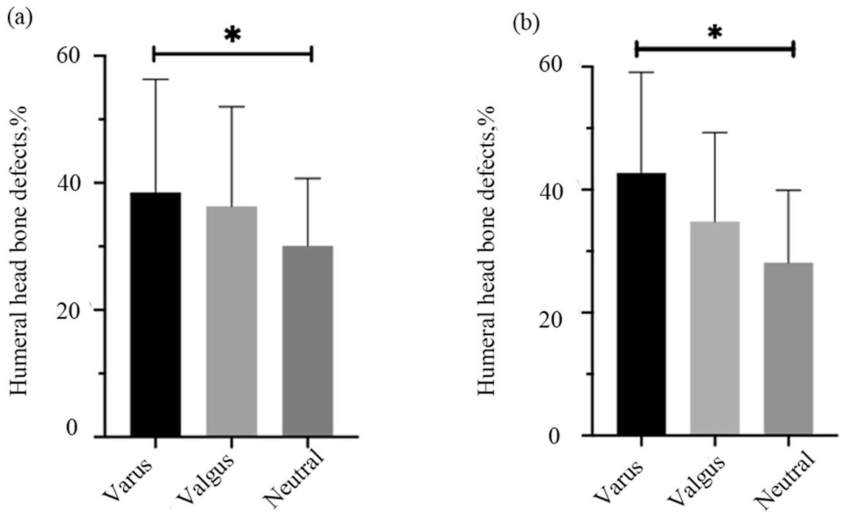

Fig. 5. Percentage of humeral head bone loss in patients with varus displaced, valgus displaced and neutral PHFs. (a), all patients; (b), patients over 65 years of age.

Table 2
The associations between percentage of humeral head bone void and facture patterns.

	Humeral head bone void percentage(%, mean ± sd)	P
Dislocation		0.23
Yes	31.1 ± 13.8	
No	37.0 ± 16.5	
Neer classification		
Neer two	31.7 ± 8.2	0.57
Neer three	35.1 ± 16.3	
Neer four	38.1 ± 16.9	

previous studies, we corroborated that the incidence rate of calcar fracture fragment was higher in varus than valgus and neutral angulated PHFs. Our study also underscored the critical role of bone mineralization within the humeral head in maintaining fracture stability, particularly in patients with osteoporotic or otherwise compromised bone structure. Through a detailed analysis of preoperative CT scans, we observed that patients exhibiting substantial bone voids within the humeral head were at an increased risk of varus displacement. This finding suggested that conventional fixation methods may be insufficient in such cases. As a result, our data advocated for a more nuanced approach to surgical planning, where the assessment of bone quality and void presence became an integral component of the preoperative evaluation. Specifically, the incorporation of bone grafting techniques within the humeral head region may be necessary to ensure adequate structural support and to mitigate the risk of fracture displacement or non-union. This approach could be particularly beneficial in older patients or those with significant bone mineral density loss, where the standard fixation might not provide the required biomechanical stability.

In their recent work, Russo and colleagues put forth a novel control volume theory and an innovative classification of PHFs [22,26]. Specifically, they developed a three-dimensional reconstruction system that partitioned the proximal humerus into four distinct regions: the greater tuberosity, lesser tuberosity, anterior calcar, and posterior calcar. Their investigation focused on the relationship between volumetric loss and head displacement in the varus or valgus, with their findings revealing that such displacement is contingent upon the balance of volumetric loss between the medial or lateral area. Notably, the authors identified a critical gap in prior research, which largely overlooked humeral bone head defects. Their own findings showed that when a fracture occurs in the proximal region of the humerus, the medial zone is bifurcated into two parts - the upper humeral head and lower medial calcar. Importantly, even if the medial calcar remains intact and sufficiently robust, significant bone defects in the humeral head can undermine effective support of the head, leading to displacement.

In this study, it was observed that bone defects in the medial or lateral part of the humeral head can lead to varus or valgus deformity, which causes the humeral head to rotate inwards or outwards. The location of the defects was found to be a significant factor in maintaining the humeral head position. The study also investigated the percentage differences between varus and valgus-displaced proximal humeral fractures PHFs and found them to be comparable. The authors hypothesized that the percentage of bone defects would be higher in varus-displaced PHFs with an intact calcar compared to those with a calcar fracture fragment. However, the differences between the two groups were not statistically significant. The mean percentage of humeral head bone void without a calcar fracture fragment was found to be 29.6 %, which indicates the minimal bone void requirements for effective head support. Nevertheless, we note that the number of samples in this study was limited, and thus a reliable threshold needs to be accurately defined in further research.

Voids in the cancellous bone weaken the structural strength and stability of the bone. When there is significant bone loss, forming noticeable voids, the bone's ability to provide support is greatly reduced. In cases of severe bone loss, augmentation with allograft fibula is recommended for stable support and satisfactory postoperative shoulder functions. However, the estimation of bone defects using mathematical equations based on 2D images has proven to be unreliable. To address this issue, this study utilized Mimics software to reconstruct premorbid 3D models of PHFs and applied Boolean subtraction to accurately calculate humeral head bone void. We suggest that the 3D reconstruction methods employed in this study can be extended to other research areas that focus on bone defects or necrosis.

The present study had certain limitations that warrant discussion. Firstly, the CT DICOM data had limited accuracy and could not show some spongial bone, which resulted in an overestimation of the bone void of the humeral head. Besides, it is also important to note that spongial bone with lower CT values below the spongial threshold has minimal contribution to humeral head support from a biomechanical standpoint. Furthermore, the factors influencing humeral head angulation are multifaceted, and the current study only accounted for the bony structure of the proximal humerus while disregarding the roles of the medial soft tissue envelope. In the future, we will further confirm the influence of humeral head bone defects on humeral head deformity and stability by measuring the bone defect of the humerus head and the medial calcar bone defects in detail before surgery, strictly grasping the length and position of screw insertion during the operation, and observing the fracture healing and secondary displacement and deformity of the humeral head through postoperative follow-up.

5. Conclusion

All types of angulation patterns exhibited humeral head bone void to some extent, with the varus-displaced PHFs demonstrating more obvious defects in comparison to the neutral angulated type.

Ethics statement

Our study was conducted in accordance with the ethical principles outlined in the Declaration of Helsinki. The research protocol was reviewed and approved by the Institutional Review Board of Peking University People's Hospital, Sichuan Panzhihua Hospital, and Fuzhou Hospital (2020PHB072-01).

Consent for publication

All authors have checked the manuscript and have agreed to the submission.

Funding

This work was financially supported by the National Science Foundation (82102553) and Peking University People's Hospital Scientific Research Development Funds (RDL2021-08 and RDE2023-21).

Data availability statement

The data were available from the corresponding upon request.

CRediT authorship contribution statement

Jiabao Ju: Writing – original draft, Methodology, Investigation, Formal analysis, Conceptualization. **Yongwen Zhou:** Writing – original draft, Methodology, Investigation, Formal analysis, Conceptualization. **Liang Chen:** Visualization, Methodology, Investigation, Formal analysis, Conceptualization. **Mingtai Ma:** Writing – original draft, Methodology, Formal analysis, Data curation. **Yichong Zhang:** Validation, Methodology, Formal analysis. **Zhentao Ding:** Validation, Methodology, Investigation, Formal analysis. **Renbin Li:** Writing – review & editing, Visualization, Methodology, Investigation, Formal analysis. **Jianhai Chen:** Writing – review & editing, Methodology, Formal analysis, Data curation, Conceptualization.

Declaration of competing interest

The authors declare that they have no known competing financial interests or personal relationships that could have appeared to influence the work reported in this paper.

References

[1] S.J. Mease, M.J. Kraeutler, D.C. Gonzales-Luna, J.M. Gregory, M.J. Gardner, A.M. Choo, Current controversies in the treatment of geriatric proximal humeral fractures, J Bone Joint Surg Am 103 (9) (2021) 829–836, https://doi.org/10.2106/JBJS.20.00665.
[2] A.P. Launonen, V. Lepola, A. Saranko, T. Flinkkila, M. Laitinen, V.M. Mattila, Epidemiology of proximal humerus fractures, Arch Osteoporos 10 (2015) 209, https://doi.org/10.1007/s11657-015-0209-4.
[3] V.K. Kancherla, A. Singh, O.A. Anakwenze, Management of acute proximal humeral fractures, J. Am. Acad. Orthop. Surg. 25 (1) (2017) 42–52, https://doi.org/10.5435/JAAOS-D-15-00240.
[4] A. Schumaier, B. Grawe, Proximal humerus fractures: evaluation and management in the elderly patient, Geriatr. Orthop. Surg. Rehabil. 9 (2018) 2151458517750516, https://doi.org/10.1177/2151458517750516.
[5] H.H. Handoll, J. Elliott, T.M. Thillemann, P. Aluko, S. Brorson, Interventions for treating proximal humeral fractures in adults, Cochrane Database Syst. Rev. 6 (2022) CD000434, https://doi.org/10.1002/14651858.CD000434.pub5.
[6] G.M. Calori, M. Colombo, M.S. Bucci, P. Fadigati, A.I. Colombo, S. Mazzola, V. Cefalo, E. Mazza, Complications in proximal humeral fractures, Injury 47 (Suppl 4) (2016) S54–S58, https://doi.org/10.1016/j.injury.2016.07.039.
[7] N. Habib, P. Fornaciari, G. Thuerig, M. Maniglio, M. Tannast, P. Vial, Hinge plate technique for osteosynthesis of comminuted proximal humeral fractures, Injury 52 (8) (2021) 2292–2299, https://doi.org/10.1016/j.injury.2021.05.005.
[8] C.E. Capriccioso, J.D. Zuckerman, K.A. Egol, Initial varus displacement of proximal humerus fractures results in similar function but higher complication rates, Injury 47 (4) (2016) 909–913, https://doi.org/10.1016/j.injury.2016.01.021.
[9] M.T. Little, M.B. Berkes, P.C. Schottel, L.E. Lazaro, L.E. Lamont, N.C. Pardee, J.T. Nguyen, D.L. Helfet, D.G. Lorich, The impact of preoperative coronal plane deformity on proximal humerus fixation with endosteal augmentation, J. Orthop. Trauma 28 (6) (2014) 338–347, https://doi.org/10.1097/BOT.0000000000000012.
[10] S.P. Dasari, B. Kerzner, L.M. Fortier, P.M. Rea, B.M. Bodendorfer, J. Chahla, G.E. Garrigues, N.N. Verma, Improved outcomes for proximal humerus fracture open reduction internal fixation augmented with a fibular allograft in elderly patients: a systematic review and meta-analysis, J. Shoulder Elbow Surg. 31 (4) (2022) 884–894, https://doi.org/10.1016/j.jse.2021.11.004.
[11] S.H. Lee, S.S. Han, B.M. Yoo, J.W. Kim, Outcomes of locking plate fixation with fibular allograft augmentation for proximal humeral fractures in osteoporotic patients: comparison with locking plate fixation alone, Bone Joint Lett. J 101-B (3) (2019) 260–265, https://doi.org/10.1302/0301-620X.101B3.BJJ-2018-0802.R1.
[12] S.W. Jung, S.B. Shim, H.M. Kim, J.H. Lee, H.S. Lim, Factors that influence reduction loss in proximal humerus fracture surgery, J. Orthop. Trauma 29 (6) (2015) 276–282, https://doi.org/10.1097/BOT.0000000000000252.
[13] H. Kantharaju, S.K. Gawhale, G.S. Prasanna Kumar, B. Sahare, N. Shah, Factors influencing the varus deformity of humeral head in proximal humerus fractures and its relation to functional outcome, Indian J. Orthop. 55 (3) (2021) 702–707, https://doi.org/10.1007/s43465-020-00275-4.
[14] Q. Yu, Z. Li, J. Li, Q. Yu, L. Zhang, D. Liu, M. Zhang, P. Tang, Calcaneal fracture maps and their determinants, J. Orthop. Surg. Res. 17 (1) (2022) 39, https://doi.org/10.1186/s13018-022-02930-y.
[15] B. Zhang, H. Lu, Y. Quan, Y. Wang, H. Xu, Fracture mapping of intra-articular calcaneal fractures, Int. Orthop. 47 (1) (2023) 241–249, https://doi.org/10.1007/s00264-022-05622-8.
[16] Y. Yin, R. Zhang, Z. Hou, S. Fan, Y. Zhuang, C. Yi, H. Chen, Y. Zhang, Fracture mapping of both-column acetabular fractures, J. Orthop. Trauma 36 (5) (2022) e189–e194, https://doi.org/10.1097/BOT.0000000000002280.
[17] J. Ju, M. Ma, Y. Zhang, Z. Ding, Z. Fu, J. Chen, Fracture line morphology of greater tuberosity fragments of neer three- and four-Part Proximal humerus fractures, Orthop. Surg. 15 (8) (2023 Aug) 1959–1966, https://doi.org/10.1111/os.13523.
[18] B.M. Armitage, C.A. Wijdicks, I.S. Tarkin, L.K. Schroder, D.J. Marek, M. Zlowodzki, P.A. Cole, Mapping of scapular fractures with three-dimensional computed tomography, J Bone Joint Surg Am 91 (9) (2009) 2222–2228, https://doi.org/10.2106/JBJS.H.00881.
[19] E. Hong, D.S. Kwak, I.B. Kim, Morphometric evaluation of detailed asymmetry for the proximal humerus. Korean Population, Multidisciplinary Digital Publishing Institute, 2021, 5.
[20] J. Jeong, J. Bryan, J.P. Iannotti, Effect of a variable prosthetic neck-shaft angle and the surgical technique on replication of normal humeral anatomy, J Bone Joint Surg Am 91 (8) (2009) 1932–1941, https://doi.org/10.2106/JBJS.H.00729.
[21] M.L. Pearl, S. Kurutz, R. Postachini, Geometric variables in anatomic replacement of the proximal humerus: how much prosthetic geometry is necessary? J. Shoulder Elbow Surg. 18 (3) (2009) 366–370.
[22] R. Russo, A. Guastafierro, L.R. Pietroluongo, A morphovolumetric study of head malposition in proximal humeral fractures based on 3-dimensional computed tomography scans: the control volume theory, J. Shoulder Elbow Surg. 27 (5) (2018) 940–949, https://doi.org/10.1016/j.jse.2017.12.004.
[23] H. Cheng, J. Yu, Z. Dong, H. Lin, Q. Liu, X. Zhang, J. Wu, X. Zeng, W. Yu, B. Xu, Treatment of 2-Part Proximal humeral fractures in osteoporotic patients with medial calcar instability using a philos plate plus an allogeneic fibula inserted obliquely - a retrospective study, Geriatr. Orthop. Surg. Rehabil. 12 (2021) 21514593211050155, https://doi.org/10.1177/21514593211050155.

[24] Q. Wang, N. Sheng, B. Rui, Y. Chen, The neck-shaft angle is the key factor for the positioning of calcar screw when treating proximal humeral fractures with a locking plate, Bone Joint Lett. J 102-B (12) (2020) 1629–1635, https://doi.org/10.1302/0301-620X.102B12.BJJ-2020-0070.R1.
[25] E.M. Padegimas, G. Chang, K. Namjouyan, S. Namdari, Failure to restore the calcar and locking screw cross-threading predicts varus collapse in proximal humerus fracture fixation, J. Shoulder Elbow Surg. 29 (2) (2020) 291–295, https://doi.org/10.1016/j.jse.2019.06.014.
[26] R. Russo, A. Guastafierro, G.D. Rotonda, S. Viglione, M. Ciccarelli, M. Mortellaro, P. Minopoli, F. Fiorentino, L.R. Pietroluongo, A new classification of impacted proximal humerus fractures based on the morpho-volumetric evaluation of humeral head bone loss with a 3D model, J. Shoulder Elbow Surg. 29 (10) (2020) e374–e385, https://doi.org/10.1016/j.jse.2020.02.022.